Article

Current Biology

Effective Modulation of Male Aggression through Lateral Septum to Medial Hypothalamus Projection

Graphical Abstract

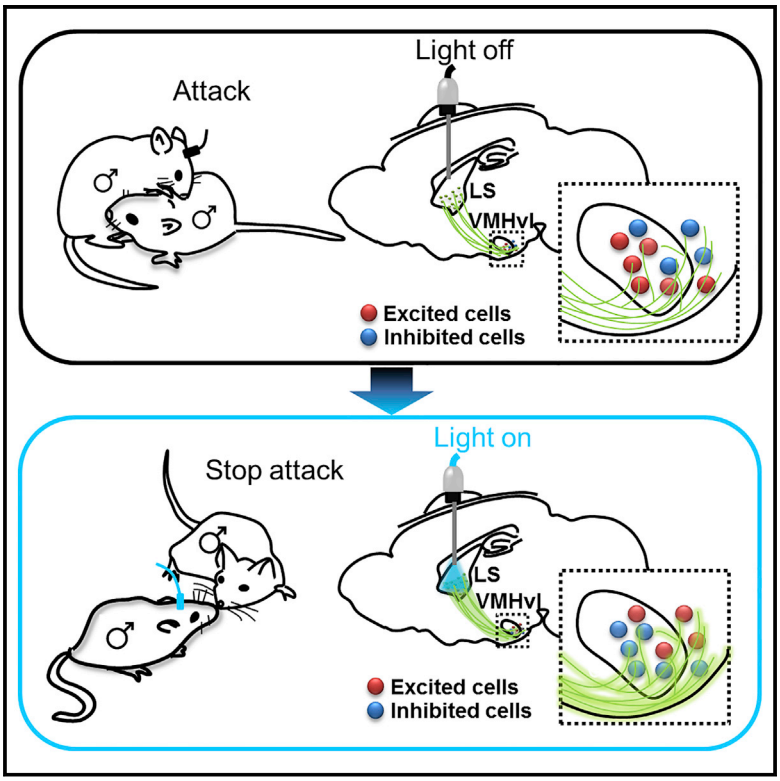

Authors

Li Chin Wong, Li Wang, James A. D'Amour, ..., James E. Feng, Robert C. Froemke, Dayu Lin

Correspondence

dayu.lin@nyumc.org

In Brief

Lesioning the lateral septum (LS) causes exaggerated aggression. Wong et al. find that LS sends direct inhibition to the ventromedial hypothalamus, ventrolateral part, a region essential for male mouse aggression. This input can effectively suppress ongoing aggression by shifting the activity balance between attack-inhibited and attack-excited cells.

Highlights

- Inhibiting LS increases aggression, whereas its activation suppresses ongoing attack
- Activating the LS-VMHvl projection inhibits attack but not mounting behaviors
- LS sends monosynaptic GABAergic inputs to the VMHvl glutamatergic cells
- The LS-VMHvl pathway inhibits attack-excited cells but activates attack-inhibited cells

Wong et al., 2016, Current Biology *26*, 1–12
March 7, 2016
http://dx.doi.org/10.1016/j.cub.2015.12.065

CellPress

Please cite this article in press as: Wong et al., Effective Modulation of Male Aggression through Lateral Septum to Medial Hypothalamus Projection, Current Biology (2016), http://dx.doi.org/10.1016/j.cub.2015.12.065

Current Biology
Article

CellPress

Effective Modulation of Male Aggression through Lateral Septum to Medial Hypothalamus Projection

Li Chin Wong,[1] Li Wang,[1] James A. D'Amour,[1,3] Tomohiro Yumita,[1] Genghe Chen,[1] Takashi Yamaguchi,[1] Brian C. Chang,[1] Hannah Bernstein,[1,2,4] Xuedi You,[1] James E. Feng,[1] Robert C. Froemke,[1,3,5] and Dayu Lin[1,2,5,*]
[1]Institute of Neuroscience, New York University School of Medicine, New York, NY 10016, USA
[2]Department of Psychiatry, New York University School of Medicine, New York, NY 10016, USA
[3]Skirball Institute of Biomolecular Medicine and Department of Otolaryngology, New York University School of Medicine, New York, NY 10016, USA
[4]The Nathan Kline Institute for Psychiatric Research, Orangeburg, NY 10962, USA
[5]Center for Neural Science, New York University, New York, NY 10003, USA
*Correspondence: dayu.lin@nyumc.org
http://dx.doi.org/10.1016/j.cub.2015.12.065

SUMMARY

Aggression is a prevalent behavior in the animal kingdom that is used to settle competition for limited resources. Given the high risk associated with fighting, the central nervous system has evolved an active mechanism to modulate its expression. Lesioning the lateral septum (LS) is known to cause "septal rage," a phenotype characterized by a dramatic increase in the frequency of attacks. To understand the circuit mechanism of LS-mediated modulation of aggression, we examined the influence of LS input on the cells in and around the ventrolateral part of the ventromedial hypothalamus (VMHvl)—a region required for male mouse aggression. We found that the inputs from the LS inhibited the attack-excited cells but surprisingly increased the overall activity of attack-inhibited cells. Furthermore, optogenetic activation of the projection from LS cells to the VMHvl terminated ongoing attacks immediately but had little effect on mounting. Thus, LS projection to the ventromedial hypothalamic area represents an effective pathway for suppressing male aggression.

INTRODUCTION

Aggression is a fundamental means to defend territory, compete for mates and food, and protect offspring. However, fighting is physically demanding and can result in severe injury or death. Thus, an active neural mechanism is in place to gate the expression of aggression. Evidence for the existence of such an aggression control system was first demonstrated by Cannon and Bard through a knife-cut experiment in cats [1]. Transections between the cortical area and hypothalamus caused excessive rage responses, such as hissing and paw striking. However, if the cut was positioned posterior to the hypothalamus, no such behaviors were observed. These results indicated that the hypothalamus is necessary for the expression of aggression and that it is under the tonic inhibition of anterior structures in the brain. Subsequent studies suggested that the septal area might mediate such control [2]. Immediate early gene mapping revealed a negative correlation between lateral septum (LS) activity and aggressive behaviors such that hyper-aggressive animals show low activity in the LS [3]. Human patients with septal forebrain tumors experience an elevated level of irritability and aggressiveness [4]. In birds and rodents, permanent lesion or pharmacological inactivation of the LS, especially the rostral part, dramatically increases the number of attacks toward conspecifics [5–11]. Conversely, electrical stimulation of the LS suppresses natural and artificially evoked aggression [12, 13]. Thus, the LS appears to be an essential gatekeeper for expression of aggressive behavior.

How does the LS modulate aggression? To answer this question, we considered the connections of the LS. Tracing studies have revealed that most LS projections end in the medial hypothalamus [14]. These projections can strongly influence the activities of medial hypothalamic neurons, as shown by the high percentage of orthodromic responsive cells in the medial hypothalamus upon LS electric stimulation [15]. The medial hypothalamus has long been recognized as a region essential for mediating aggression [16–19]. Electric stimulation of the "hypothalamic attack area," which overlaps with multiple medial hypothalamic nuclei, induces attack in both rats and cats [16, 19]. More recently, we and others pinpointed a subnucleus in the medial hypothalamus, the ventromedial hypothalamus ventrolateral area (VMHvl), as a locus required for attack in male mice. Silencing the VMHvl or killing progesterone receptor (PR)-expressing cells in the VMHvl abolished naturally occurring inter-male attack, while optogenetic stimulation of the VMHvl elicited immediate attack toward males, females, and inanimate objects [20–22]. Chronic in vivo recording further demonstrated that VMHvl cells are active during natural inter-male aggression, and that they signal the imminence and features of future attacks [23]. Based on these observations, we hypothesized that the LS might modulate aggression by influencing the activities of attack-related cells in the medial hypothalamus, especially those in and around the VMHvl. To test this, here we optogenetically activated the LS-VMH pathway; we found that this manipulation suppressed attack effectively but had little effect on male-female mounting. Furthermore, we performed optrode recording in socially interacting animals and found that LS inputs decreased the activity of attack-excited cells but surprisingly increased the activity of attack-inhibited cells. Thus, the pathway from

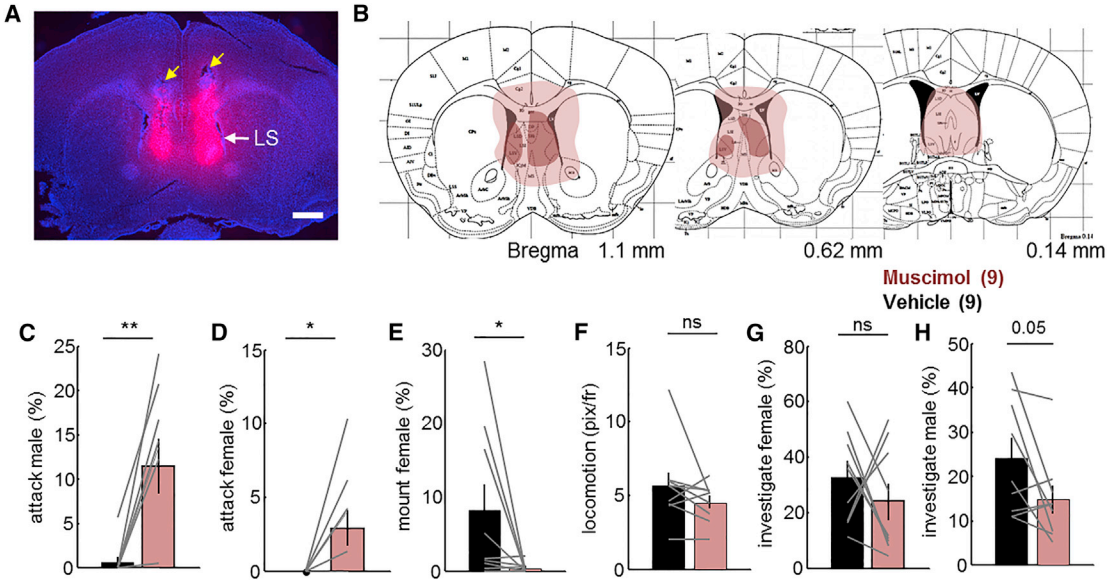

Figure 1. Inhibition of the Lateral Septum Increases Aggression toward Male and Female Intruders

(A) A coronal section showing an example of fluorescent muscimol (red) spread in the lateral septum (LS). Blue, DAPI. Scale bar, 0.5 mm.

(B) Extent of drug spread. Dark red indicates the animal with the least spread; light red indicates the animal with the largest spread.

(C) Muscimol injection into the LS increased the total percentage of time spent attacking male intruders.

(D and E) Muscimol injection into the LS increased the total percentage of time spent attacking female intruders (D) and abolished mounting behavior (E).

(F–H) Muscimol injection into the LS did not affect locomotion (F) or incidence of investigation of females (G) but decreased incidence of investigation of males (H).

Error bars show ±SEM. Gray lines indicate individual animals. N = 9. Paired t test or Wilcoxon signed-rank test for non-normally distributed data. *$p < 0.05$. **$p < 0.01$.

the LS to the VMHvl and its surrounding areas represents an effective route for controlling aggressive behavior.

RESULTS

LS Suppression Increases Aggression toward Both Males and Females

"Septal rage" has been described in several rodent species [5–8]. However, in male mice, this rage phenotype has only been reported after LS electric lesion that damages both cell bodies and fibers of passage [6]. Thus, we infused the $GABA_A$ receptor agonist muscimol (0.2–0.3 μl of 0.33 mg/ml) into the LS to determine whether the LS-lesion-induced rage response can be recapitulated in male mice by inactivating LS cells alone (Figures 1A and 1B). Males with relatively low aggression level (total attack time < 5 s during the 10 min resident-intruder assay) were used in the test to avoid behavioral saturation. 30 min after muscimol infusion, we performed the resident-intruder assay for approximately 20 min, first with male intruders (10 min) and then with female intruders (10 min). Consistent with previous lesion studies [6], we observed a significant increase in attack after LS inactivation (Figures 1C and 1D). After the vehicle injection, only 1/9 animals attacked the male intruder, whereas 8/9 animals initiated attack after muscimol infusion (Figure 1C). More dramatically, although male residents typically initiate sexual behavior toward females, 5/9 mice attacked females repeatedly after the LS inactivation, while mounting behavior was nearly abolished (Figures 1D and 1E). This increased aggression was not accompanied by a general increase in arousal, as locomotion did not significantly change between attacks (Figure 1F). Whereas the time spent investigating females did not change significantly after the muscimol injection, the male investigation time decreased, possibly due to increased time of attack ($p = 0.05$, paired t test; Figures 1G and 1H). Thus, muscimol inhibition of LS cells increases aggression in male mice toward both male and female conspecifics.

Optogenetic Activation of the LS Suppresses Social Behaviors

As a complementary approach to the loss-of-activity manipulation, we next tested the effect of the LS activation on aggressive behaviors (Figure 2A). To activate LS cells, we stereotaxically injected adeno-associated virus (AAV) expressing channelrhodopsin-2 fused with yellow fluorescent protein (ChR2-EYFP) into the LS in wild-type animals (N = 16) and implanted an optic fiber 0.5 mm above the LS (Figures 2B and 2D). During the surgery, a virus expressing LacZ or tdTomato was co-injected to help locate the infected cell bodies histologically. We found that 90.2% ± 3.2% (mean ± SE) of LacZ- or tdTomato-expressing cells were located inside of the LS (Figure 2C). Scattered infected cells (ranging from 0% to 34%) were observed in regions outside of the LS, but mostly in the median septum (MS) (Figures 2C and 2D). Figure S1 shows the full range of infection from an example animal. After 3 weeks of viral incubation, we delivered 473 nm blue light (20 ms, 20 Hz, 1–3 mW) through the optic fibers to activate the LS cell bodies during male-male interaction. Given that light stimulation is expected to reduce aggression, we started stimulation immediately after an attack was initiated and continued

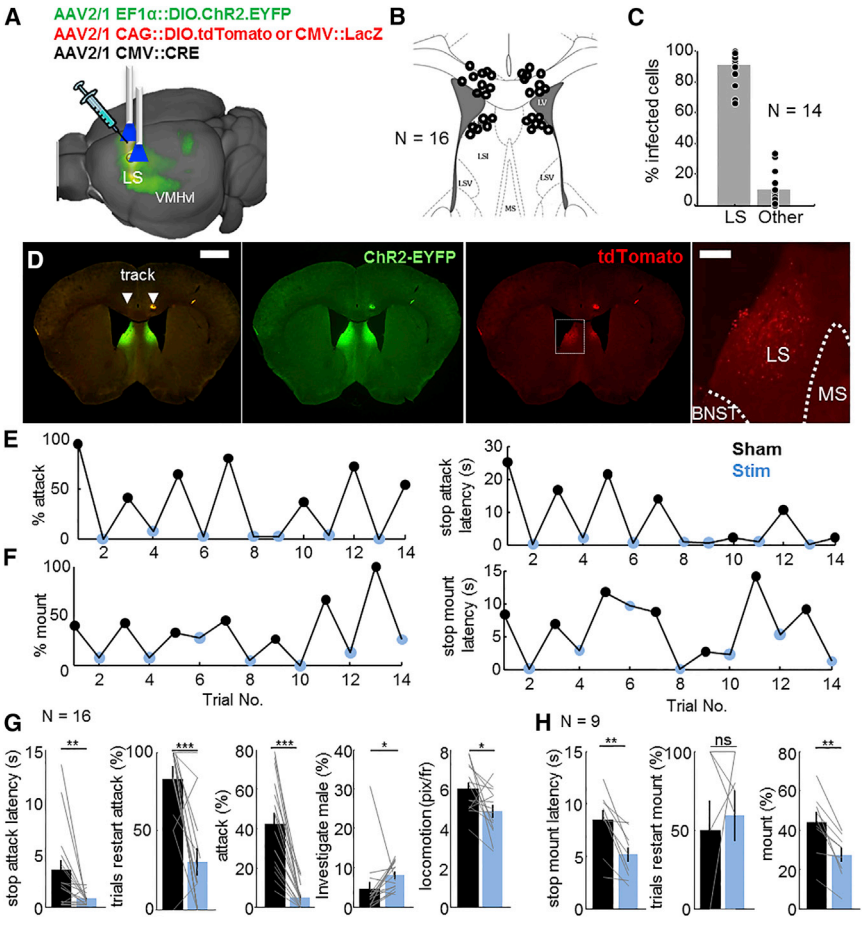

Figure 2. Optogenetic Activation of the LS Suppresses Aggressive Behaviors

(A) Viral injection and light stimulation in the LS. Image is adopted and modified from http://connectivity.brain-map.org/ experiment 100141435, which shows the GFP signal after injecting AAV2/1 hSynapsin.EGFP.WPRE.bGH into the LS region.

(B) Cannula positions in animals that were included in the analysis. Each circle represents one animal. N = 16.

(C) Over 90% of LacZ or tdTomato cells were found in the LS. "Other" refers to all regions outside the LS, although most non-LS infected cells were located in the medial septum (MS). N = 14.

(D) A coronal section shows endogenous ChR2-EYFP (green) and tdTomato (red) expression in the LS and cannula ending points (arrowheads). Scale bars, 0.2 mm for the rightmost image and 1 mm for the remaining images. The rightmost image shows an enlarged view of the boxed area in the image second from right. BNST: bed nucleus of stria terminalis.

(E) Percentage of time spent in attack (left) and stop attack latency (right) in one session from one example animal with interleaved stimulation trials (blue) and sham trials (black).

(F) Same conventions as (E), showing results from an example session with a female intruder.

(G) In comparison to sham epochs (black bars), during LS light stimulation (blue bars) test animals significantly reduced latency to stop attack, decreased probability to re-initiate attack, decreased percentage of time spent in attack, increased amount of time spent investigating male intruders, and decreased locomotion during non-attack epochs. N = 16.

(H) When encountering a female, LS optogenetic stimulation significantly decreased the latency to stop mounting but did not change the probability of mounting re-initiation. The total amount of time animal spent in mounting significantly decreased. N = 9.

Error bars show ±SEM. Gray lines represent individual animals. Paired t test or Wilcoxon signed-rank test for non-normally distributed data. *$p < 0.05$, **$p < 0.01$, ***$p < 0.001$. See also Figures S1 and S2.

the light delivery for 20 s. Sham stimulations (20 ms, 20 Hz, 0 mW for 20 s) were interleaved with real stimulations to account for natural self-termination of attack (Figure 2E).

Acute activation of LS cells was highly efficient in terminating attack. During light stimulation, animals stopped ongoing attack with significantly shorter latency (sham: 3.5 ± 1.0 s, light: 0.7 ± 0.1 s, mean ± SE, $p = 0.004$) and were much less likely to reinitiate attack (sham: 82.9% ± 7.7%, light: 29.6% ± 8.9%, $p = 0.0005$; Figures 2E and 2G). As a result, the total amount of time spent in attack was only 10% of that during sham stimulation (sham: 42.1% ± 5.8%, light: 4.6% ± 1.4%, $p = 4.8 \times 10^{-6}$; Figures 2E and 2G). The stimulated animals remained highly interested in the male intruder, and in fact they spent more time investigating the intruder during the real stimulation than during the sham stimulation (sham: 4.4% ± 1.9%, light: 7.9% ± 0.9%, $p = 0.02$; Figure 2G). Although the animal continuously moved around the cage, locomotion during the non-attack period significantly decreased ($p = 0.03$; Figure 2G). In addition, in nine animals that achieved intromission during interaction with females, the LS stimulation mildly but significantly decreased the latency to stop mounting (sham: 8.4 ± 1.0 s, light: 5.1 ± 0.8 s, $p = 0.002$) and reduced the total percentage of time spent mounting (sham: 43.7% ± 5.1%, light: 27.1% ± 3.7%, $p = 0.001$), although the probability of reinitiating mounting did not change significantly (sham: 50.0% ± 18.9%, light: 59.2% ± 16.2%, $p = 0.61$; Figures 2F and 2H). Thus, LS activation strongly suppressed aggression but also caused behavioral changes not related to aggression. In control animals that expressed EGFP instead of ChR2-EYFP in the LS, light activation of the LS did not significantly change locomotion, attack, or social investigation (Figures S2A–S2C).

Optogenetic Activation of the LS-VMH Projection Suppresses Fighting but Not Mounting Behavior

Histological analysis revealed that dense ChR2-EYFP fibers encapsulate the VMH in LS-targeted animals (Figures 3B and 3C; see also http://connectivity.brain-map.org/Experiment100141435). Previous Golgi studies revealed that VMHvl cells extend primary dendrites into the fiber plexus surrounding the nucleus, forming dense synapses with axons from distal brain areas [24, 25]. Given the essential role of the VMHvl in male aggression [20–22], we next tested whether the

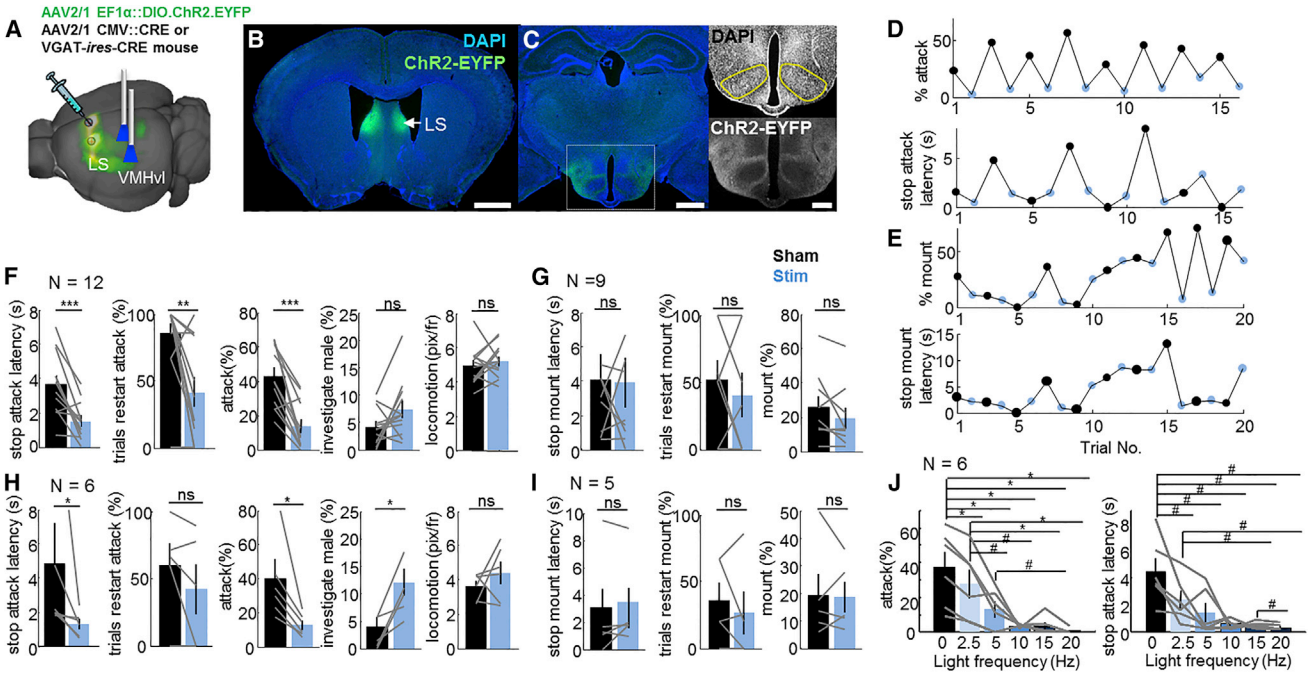

Figure 3. Optogenetic Activation of the LS Terminals at the VMH Area Suppresses Attack but Not Mounting

(A) Schematic showing viral injection into the LS and stimulation of the LS terminals in the VMHvl area.

(B) Representative coronal section showing ChR2-EYFP expression (green) in the LS. Blue, DAPI. Scale bar, 1 mm.

(C) ChR2-EYFP fibers in the medial hypothalamus amplified with YFP staining. Section is from the same animal shown in (B). Images at right show enlarged view of boxed area at left. Scale bars, 1 mm (left) and 250 μm (right).

(D) Example session shows the percentage of time spent in attack and latency to stop attack during interleaved stimulation trials (blue) and sham trials (black).

(E) Example session of interaction with a female intruder. Conventions are as in (D).

(F) In wild-type animals, LS-VMHvl stimulation significantly reduced the latency to stop attack and the probability to reinitiate attack and decreased the percentage of time spent in attack, but it did not change the percentage of time spent in male investigation and locomotion. N = 12.

(G) LS-VMHvl stimulation did not change latency to stop mounting, mounting re-initiation probability, or percentage of time spent mounting in wild-type animals. N = 9.

(H and I) LS-VMH light stimulation suppressed aggression (H, N = 6) but caused no change in mounting behavior (I, N = 5) in *Vgat*-ires-Cre animals. Paired t test or Wilcoxon signed-rank test if data is not normally distributed. *$p < 0.05$, **$p < 0.01$, ***$p < 0.001$.

(J) Decreased percentage of time spent in attack (left) and shortened attack latency (right) with increased light pulse frequency. N = 6 wild-type animals. #False discovery rate-adjusted $p < 0.1$, *$p < 0.05$. The Jarque-Bera test and Lillie test confirmed normal distribution for all groups except % attack measure for the 15 Hz and 20 Hz conditions and latency measure for the 5 Hz group. One-way ANOVA with repeated measures revealed significant difference among groups ($p < 0.0001$). A paired t test was used to compare mean values between groups if both groups were normally distributed. A signed-rank test was used if one or both groups were not normally distributed.

Error bars show ±SEM. Each gray line represents one individual animal. See also Figure S3.

suppression of aggression induced by LS activation was mediated partly through interactions with cells in or around the VMHvl. When we virally expressed ChR2 in the LS and positioned the optic fiber 0.5 mm above the VMHvl (Figure 3A; N = 12), we found that light stimulation of the LS-VMHvl pathway effectively suppressed ongoing attack. Upon light delivery, animals quickly aborted attack (stop attack latency: sham: 3.4 ± 0.6 s, light: 1.4 ± 0.3 s, $p = 0.002$) and were less likely to reinitiate the attack (attack re-initiation probability: sham: 84.9% ± 8.6%, light: 41.4% ± 11.0%, $p = 0.006$; Figures 3D and 3F). Whereas the total attack time during stimulation was approximately one-third of that during sham trials (sham: 42.1% ± 5.1%, light: 13.3% ± 3.9%, $p = 0.0001$; Figures 3D and 3F). The total investigation time ($p = 0.09$) and movement velocity during non-attack period was not significantly altered ($p = 0.51$, Figure 3F). In nine animals that achieved intromission during interaction with females, stimulation caused no change in latency to stop mounting ($p = 0.87$), total percentage of time spent in mounting ($p = 0.13$), or probability of mounting re-initiation ($p = 0.54$; Figures 3E and 3G). Given the known role of the LS in regulating anxiety [26], we tested the effect of LS and LS-VMH activation on animals' performance in an elevated plus-maze test (EPM) (Figures S2D and S2E). We interleaved the sham and real stimulation (20 s, 20 Hz, 20 ms, 1–3mW) and compared the percentage of time animal spent in the open versus closed arm under each stimulation condition. We found that LS stimulation, but not LS-VMH stimulation, increased movement velocity in the EPM, but neither manipulation changed the distribution of time in the open versus closed arms (Figures S2F and S2G). These data suggest that LS-stimulation-induced anxiogenic response [27] is likely to be long-term rather than acute and does not account for the fast suppressive effect of the LS/LS-VMH stimulation on aggression.

To determine the range of the light stimulation frequency that can influence aggression, we systematically varied the optical stimulation rate from 2.5 Hz to 20 Hz. We found that even at 2.5 Hz, stimulation of the LS-VMH terminals was sufficient to consistently reduce aggression (Figure 3J; N = 6, $p < 0.05$, paired t test). As the frequency increased, the suppression gradually became stronger and reached a plateau at 10 Hz. Although the firing properties of the LS cells during social behaviors are unknown, in vivo recordings during discrimination tasks revealed that LS spontaneous firing rate activity ranges from 2 to 5 Hz and can increase to 10–20 Hz in response to a preferred stimulus [28]. Thus, LS activation could modulate aggressive behavior at frequencies within its normal activity range.

Unlike most brain regions, which contain mixed glutamatergic and GABAergic cells, the LS contains largely GABAergic cells. To test whether long-projecting GABAergic cells in the LS mediate suppression of aggression, we expressed ChR2 in the GABAergic cells using a well-characterized transgenic line that expresses Cre recombinase in cells containing the vesicular GABA transporter (VGAT) (Figures S3A–S3C) [29]. By crossing *Vgat*-ires-Cre mice with a GFP reporter line, we found that 85.2% of cells in the LS were GFP positive (Figure S3D), consistent with the endogenous proportion of GABAergic cells in this area [30]. Upon optogenetic activation of the GABAergic projection from the LS to the VMHvl, animals (N = 6) quickly aborted ongoing attacks (sham: 4.8 ± 2.4 s, light: 1.3 ± 0.3 s, $p = 0.03$, paired t test) and reduced the total percentage of time spent attacking (sham: 40.0% ± 11%, light: 12.4% ± 2.7%, $p = 0.03$; Figure 3H). The percentage of trials to reinitiate attack did not significantly decrease during light stimulation, possibly due to the variable and lower attack re-initiation probability of *Vgat*-ires-Cre mice (Figure 3H). Whereas the locomotion velocity between attacks did not change ($p = 0.51$), the total time spent on investigation increased during stimulation ($p = 0.03$; Figure 3H). Mounting behavior against female intruders was not affected by the stimulation (stop mounting latency: $p = 0.42$, total time of mounting: $p = 0.90$, mounting re-initiation probability: $p = 0.49$, N = 5; Figure 3I).

One caveat of terminal stimulation is that it may activate cell bodies through back propagation of action potentials [31]. If axons bifurcate, the behavioral changes observed during terminal activation might result from the recruitment of a second region. To address this issue, we activated the LS-VMH pathway while simultaneously inactivating LS cell bodies with a locally injected mixture of lidocaine and tetrodotoxin (TTX) (Figures 4A–C). Before drug infusion, LS and LS-VMH stimulation effectively suppressed attack ($p < 0.05$, t test between sham and light trials for each animal), and LS stimulation caused significant decrease in locomotion ($p = 0.02$, t test, N = 6; Figures 4D–4F, LS: solid black bars; LS-VMH: open black bars). After LS drug infusion, stimulation within the LS itself failed to reduce attack or affect locomotion (Figure 4D–4F, solid red bars). In contrast, activation of LS terminals in or around the VMHvl shortened the latency to stop attack ($p = 0.02$) and reduced total attack time ($p = 0.01$) (Figures 4D and 4E, open red bars). The locomotion was not affected by the LS-VMH stimulation either before or after drug blocking (Figure 4F, open black and red bars, $p = 0.22$ and 0.87). Thus, LS input to the VMHvl area is sufficient to suppress aggression independent of LS cell body activity.

LS Input Suppresses VMHvl Cell Activity In Vitro

Given the clear suppressive effects of LS-VMHvl projection on aggression, we next examined the influence of LS input on the activity of VMHvl cells. After viral expression of ChR2 in LS neurons for 6 weeks, we first confirmed that the LS neurons could influence the activity of the VMHvl neurons in vitro. We prepared acute brain slices and made whole-cell recordings from VMHvl neurons. Given that VMH cells are almost entirely glutamatergic, transgenic mice expressing ZsGreen in glutamatergic cells were used for a subset of experiments to facilitate the identification of the VMHvl (Figure 5A) [32]. After each recording, cells were filled with biocytin and histologically confirmed to be within the boundary of the VMHvl (Figures 5B and 5C). During recording, blue light (473 nm) was applied through a 40× objective centered over the soma of the recorded neuron at either 5 or 20 Hz while cells were held at moderately depolarized values (~–40 mV). In 9/11 cells, we observed light-evoked inhibitory postsynaptic currents (IPSCs) ranging from 82 to 330 pA (blue; Figures 5D and 5E) with a latency of 3 ± 0.56 ms (mean ± SD). These currents were blocked by the $GABA_A$ receptor antagonist gabazine (1 μM; black, Figures 5D and 5E) but were unaffected by the $GABA_B$ receptor antagonist CGP (1 μM; red, Figures 5D and 5E). Given the short latency and the small jitter of light-evoked IPSCs, the recorded cells are likely to receive direct inhibitory inputs from GABAergic LS neurons.

The impact of LS input on VMHvl spiking activity was investigated by applying 500 ms inward current pulses in 50 pA increments from 0 to 400 pA either with or without blue light pulses (20 ms, 20 Hz). Across cells, light activation of LS terminals could significantly reduce spiking evoked by large current steps (paired t test, $p \leq 0.05$ for the largest three current steps) when the firing rate was relatively high (mean ± SD: 7.2 ± 5.8 spikes/s) (Figures 5F and 5H). In 8/11 cells, rebound spikes were observed after 500 ms hyperpolarizing current steps ranging from –50 pA to –500 pA (Figure 5I). Interestingly, in 7 of the 8 cells that showed rebound spiking, we observed a prominent "sag" in the voltage response to the hyperpolarizing current (Figure 5I). The magnitude of the sag was significantly correlated with the number of rebound spikes (Figure 5J), and the sag was not observed in the three cells without rebound spiking (Figure 5K), suggesting that the hyperpolarization-activated cation current (I_h) could be responsible for generating the rebound spiking.

LS Input Causes Differential Activity Changes in Attack-Excited and Attack-Inhibited Cells

To understand how the LS input might influence the in vivo activity of VMHvl cells, especially those that respond during aggression, we expressed ChR2 in the LS and implanted an optrode to record the responses of VMHvl cells during male-male interaction and during light activation of LS-VMH terminals (Figure 6A) and the LS (Figure 7A). We recorded a total of 233 units from eight animals with electrode tracks centered in the VMHvl (Figure 6B). 231 units were tested with LS-VMH stimulation, and 224 of those units were tested with LS direct stimulation.

During recording, a group-housed BALB/c male intruder was introduced into the home cage of the recorded mouse, which

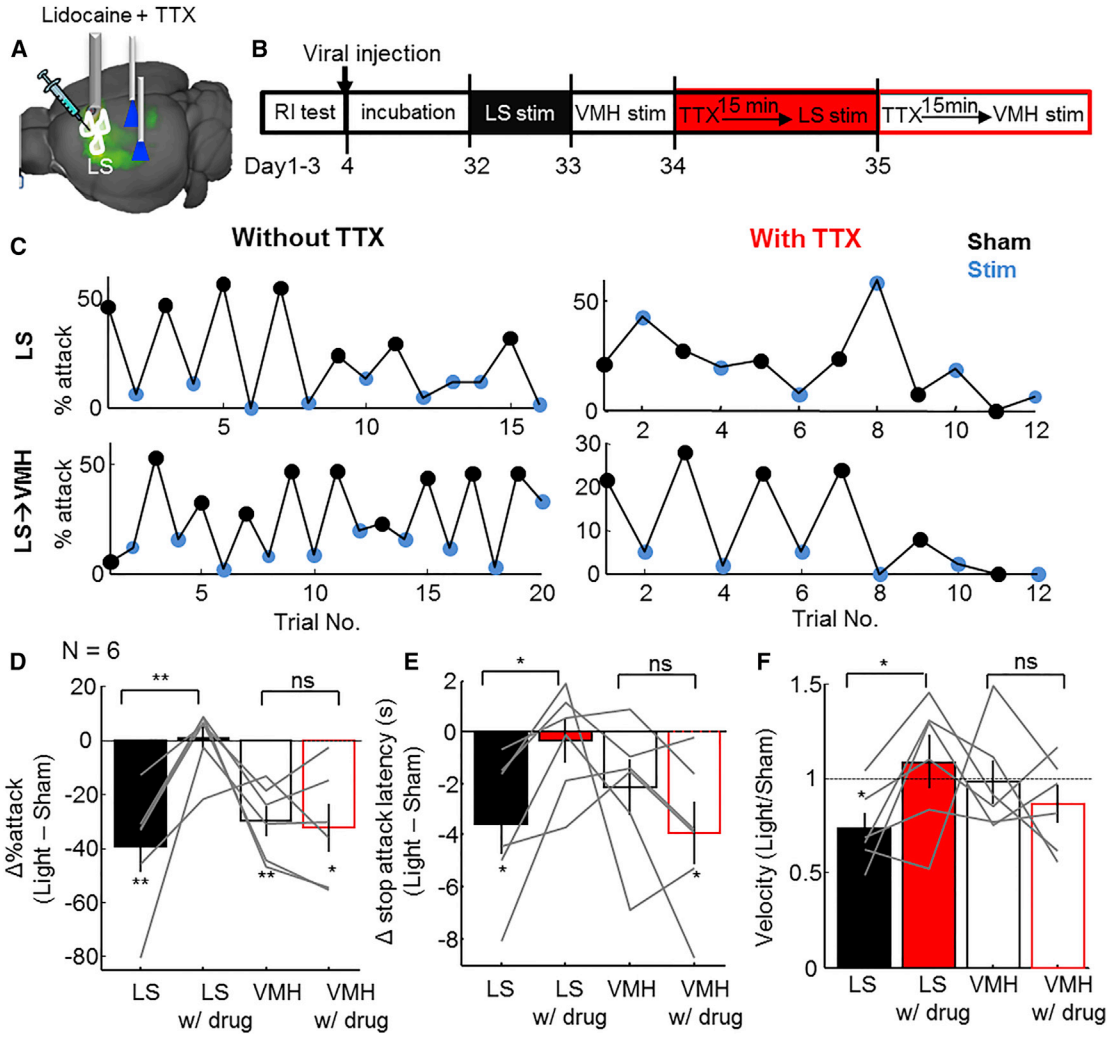

Figure 4. Activation of the LS Terminals in the VMHvl Area Suppresses Aggression Independent of LS Activity

(A) LS-VMH stimulation with a mixture of TTX and lidocaine injection into the LS.

(B) Timeline of the experiment.

(C) Both LS and LS-VMH stimulations reduced the percentage of time spent attacking before the drug injection (left). After LS blocking, LS stimulation no longer inhibited aggression (top, right), while LS-VMH stimulation did (bottom, right).

(D–F) Differences in the percentage of attack time (D), latency to attack (E), and movement velocity (F) between real and sham stimulations. Two-way ANOVA revealed significant differences between the drug conditions and sites of stimulation for all three parameters measured (D, $p = 0.008$; E, $p = 0.03$; F, $p = 0.05$). Paired t test showed a significant difference in all three parameters between before-drug and after-drug conditions for the LS stimulation but not for the VMH stimulation ($p > 0.1$). Student's t test was used to determine whether light stimulation induced significant change of the behavioral parameter from sham epochs for each test condition. Gray lines indicate individual animals. Error bars show ±SEM. N = 6. *$p < 0.05$, **$p < 0.01$.

quickly elicited approach, investigation, and repeated attacks. Among the 233 recorded units, 65 (27.9%) showed increased spiking activity during attack (averaged Z score during the last second of attack > 2), while 26 (11.2%) decreased firing rate (Z score < –2) (Figures 6C and 6D).

To examine the response of VMHvl cells to LS input, we delivered blue light pulses (5–10 times for 20 s, 5 Hz, 20 ms pulses) through the implanted optrode in the presence of a male intruder regardless of the ongoing behavior. The light delivered through the optrode was at low intensity (0.2–0.3 mW), and it did not alter aggressive behaviors significantly (Figure S4A). The 20 ms LS-VMH terminal activation induced clear activity fluctuations in the VMHvl cells, starting 8 ms after the light onset and lasting up to 70 ms post-stimulation (Figures 6E–6G). For those cells that were optically sensitive, we found that light stimulation mainly suppressed VMHvl cell activity initially (8–15 ms after light onset), with 43/231 units decreasing firing (averaged Z score peristimulus time histogram during 8–15 ms aligned to light onset < –1) and 8/231 units increased firing (averaged Z score > 1) (Figures 6F and 6G). However, between 0 to 20 ms after light offset, 72/231 units showed increased activity (averaged Z score > 1), whereas only 9/231 units showed decreased activity (averaged Z score < –1). This is surprising, as it suggests that despite receiving inhibitory

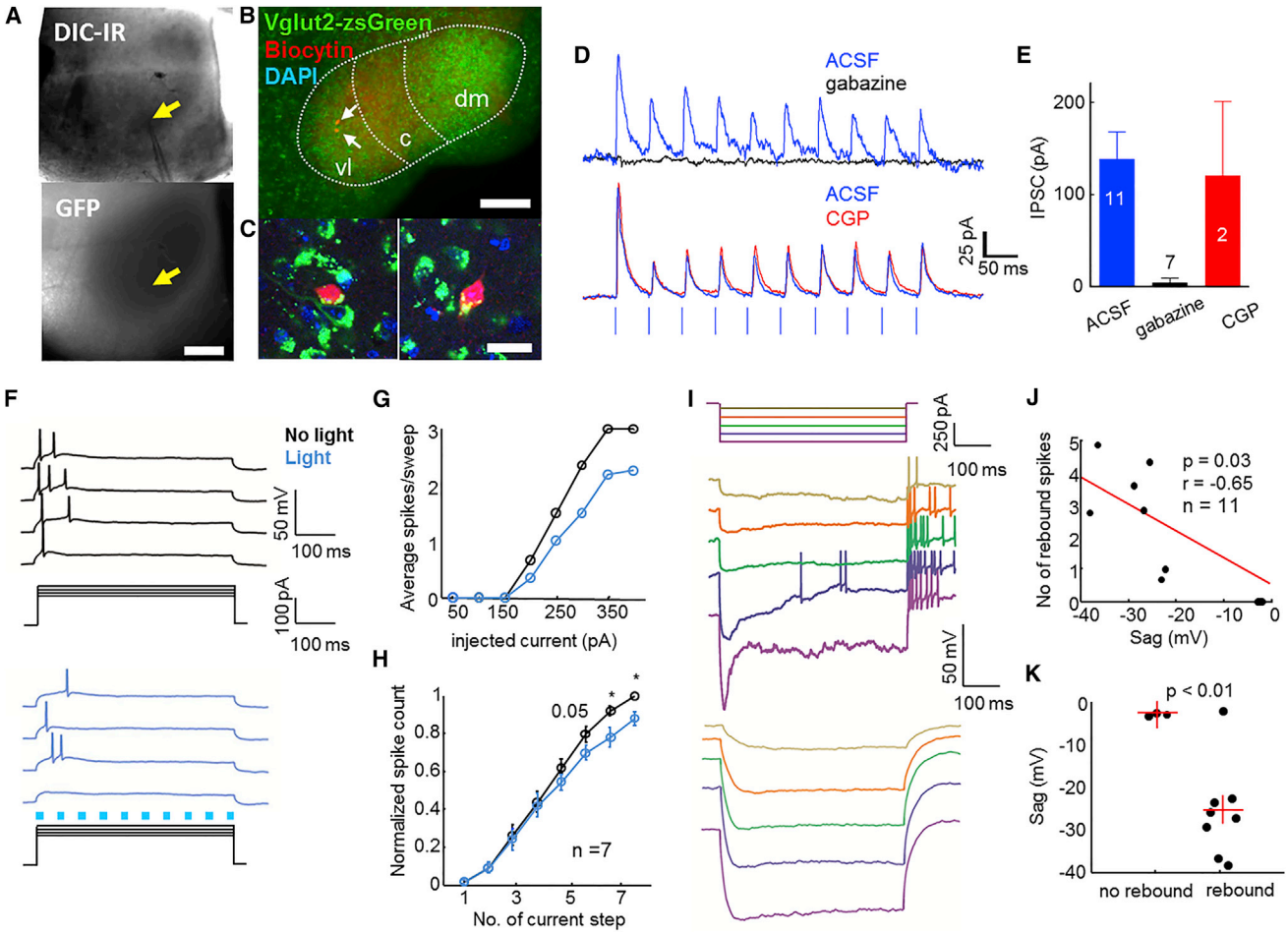

Figure 5. In Vitro Whole-Cell Recordings Reveal the GABAergic Input from the LS to the VMHvl Neurons

(A) A representative differential interference contrast image under the infrared light (top) and the corresponding image under the green fluorescent channel (bottom) from a recorded slice of a *Vglut2*-ires-Cre × Ai6 mouse. Yellow arrows indicate the pipette tip. Scale bar, 200 μm.

(B) Biocytin-filled cells (white arrows) and endogenous expression of ZsGreen in VGLUT2-positive cells.

(C) Magnified views of the red cells in (B). Both cells expressed ZsGreen and are thus glutamatergic. Scale bars in (B) and (C), 200 and 20 μm, respectively.

(D) Example traces from two different cells (blue) with light-evoked IPSCs at 20 Hz while held at –40 mV. Blue ticks indicate individual light pulses. IPSCs were blocked with the application of 1 μM gabazine (top, black), but not with 1 μM CGP ($GABA_B$ receptor blocker; bottom, red).

(E) Summary of peak amplitude of the first IPSC in ACSF (blue), gabazine (black), or CGP (red). Error bars show means ± SEM.

(F) Example traces from one cell during current steps with (blue) and without (black) simultaneous light delivery (blue ticks).

(G) Spike frequency-current plot for the cell in (F).

(H) Across all cells, blue light (blue) significantly suppressed the spiking rate when the rate was relatively high. *$p < 0.05$, paired t test.

(I) Voltage response traces from two representative cells injected with stepped outward currents. The top cell shows the sag and post-hyperpolarization rebound spikes, whereas the bottom cell does not.

(J) The average number of rebound spikes is significantly correlated with the magnitude of sag.

(K) Cells with rebound spiking (n = 3) and those without (n = 8) differ significantly in their magnitude of sag. Red crosses indicate the mean of the group.

input from the LS, VMHvl cells were actually excited rather than inhibited by the LS-VMHvl stimulation, which should have promoted attack based on our previous optogenetic activation studies in the VMHvl [20]. To further understand the effect of the optical stimulation on VMHvl attack-related cells, we examined the relationship between responses during attack and during light stimulation. We found that the early (8–15 ms) light responses were not correlated with the attack responses ($r = 0.03$, $p = 0.67$; Figure 6H), given that attack-excited and attack-inhibited units were similarly suppressed. However, the post-light excitation was significantly inversely correlated with the attack response ($r = –0.34$, $p = 8.5 \times 10^{-8}$) such that the attack-inhibited units were much more likely to show strong post-light excitation (Figure 6I). When we considered the early and late light-induced responses together, the overall light response was significantly negatively correlated with the attack responses ($r = –0.30$, $p = 3.3 \times 10^{-6}$; Figure 6J).

To understand how light stimulation affected VMHvl activity in our optogenetic experiment, we delivered blue light through a 230 μm optic fiber implanted above the LS while recording the activities of VMHvl cells during social interaction (Figure 7A). We used a light pulsing protocol (20 ms, 5 Hz, 1–3 mW) similar

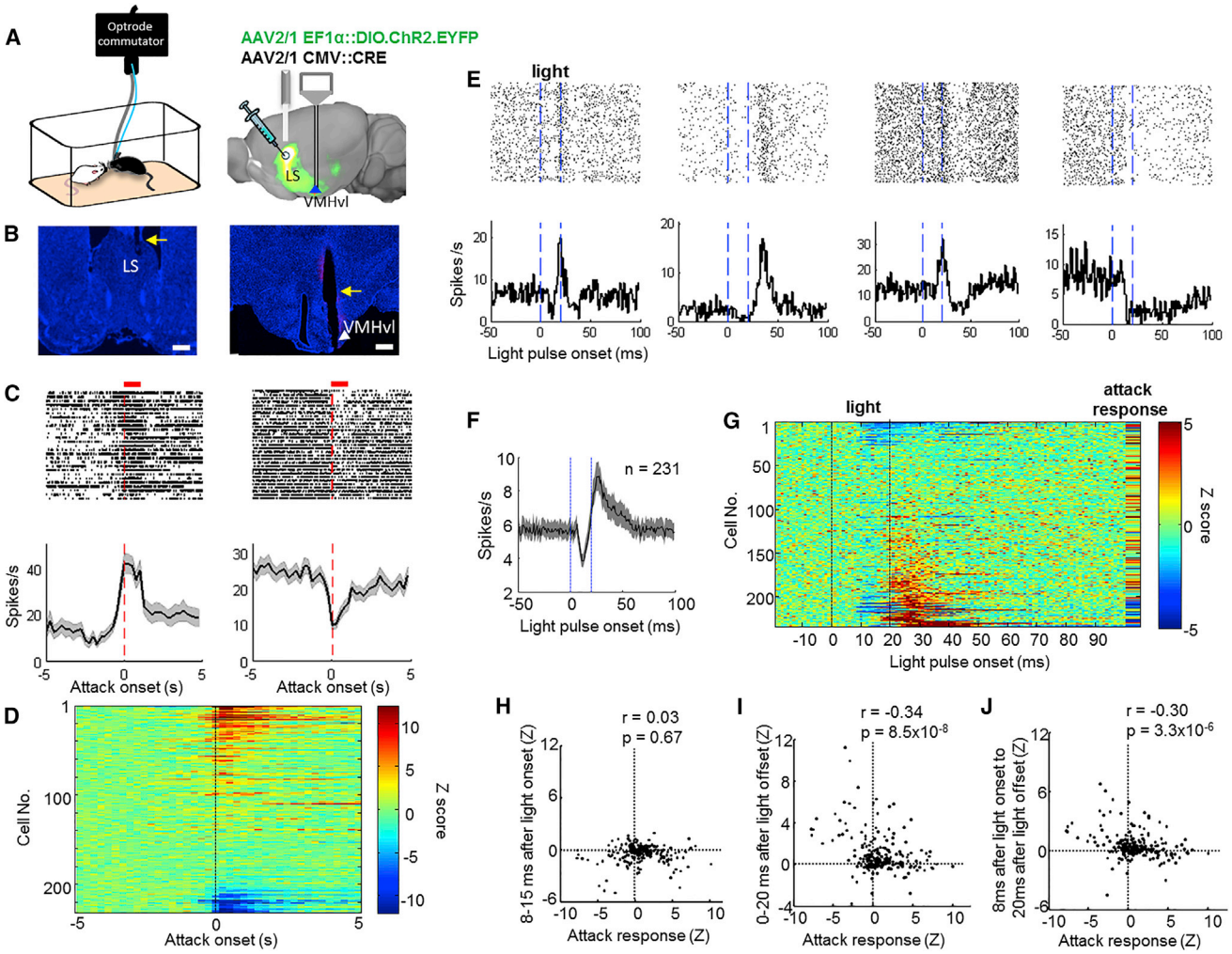

Figure 6. VMHvl Cell Responses during Attack and during LS-VMH Terminal Stimulation

(A) Optrode recording at the VMHvl with LS-VMH optical stimulation.

(B) Coronal sections show the optic fiber (yellow arrow) position in the LS (left) and the optrode track (yellow arrow) in the VMHvl (right). Blue, DAPI; red, DiI. Scale bar, 0.5 mm.

(C) Raster plots (top) and peristimulus time histograms (PSTHs) (bottom) of two representative cells aligned to attack onset. Red horizontal bars indicate the minimal attack duration (1 s) for each trial. Dashed red lines indicate time 0. Shading shows the ±SEM.

(D) Z-score-transformed PSTHs of all recorded cells aligned to attack onset. Cells are sorted in descending order based on their responses during attack.

(E) Light responses of four example cells aligned to the light onset. Blue dashed lines delimit the light-on period.

(F) Averaged PSTH aligned to light onset of all recorded VMHvl cells. Shading shows the ±SEM.

(G) Z-score-normalized activity of all 231 cells aligned to light onset, sorted based on averaged activity between 8 ms after light onset and 20 ms after light offset. Normalized activity of each cell during attack is shown on the right side of the heatmap.

(H) The immediate response to light (8–15 ms after light onset) is uncorrelated with attack response ($r = 0.03$, $p = 0.67$, Pearson's correlation).

(I) The post-light response (0–20 ms after light offset) is significantly negatively correlated with the attack response ($r = -0.34$, $p = 8.5 \times 10^{-8}$).

(J) The total light-related response (8 ms after light onset to 20 ms after light offset) is negatively correlated with attack response ($r = -0.30$, $p = 3.3 \times 10^{-6}$). See also Figure S4.

to that used in our optogenetic study, and as expected, attack decreased during light when compared with the time-matched period before light (Figure S4B). The effect of LS cell body stimulation on VMHvl activity was qualitatively similar to the LS-VMH terminal stimulation, but it had a longer delay and was much more robust (Figure 7B). Across the population, upon each 20 ms light pulse, VMHvl cells were briefly suppressed and then showed strong excitation (Figure 7C). When the 20 s light pulsing period was considered as a whole, we observed units being clearly inhibited or excited during the light delivery (Figures 7D and 7E; additional sample cells in Figures S5A–S5F). Across the population, the attack response was significantly negatively correlated with the 20 s light response ($r = -0.34$, $p = 2.6 \times 10^{-7}$) such that strong attack-excited units were more likely to be inhibited by light, whereas strong attack-inhibited units were more likely to be excited by light (Figure 7F). The mean firing rate of attack-excited cells was significantly decreased during the light stimulation (one-sample t test, $p = 0.01$, $n = 58$), whereas

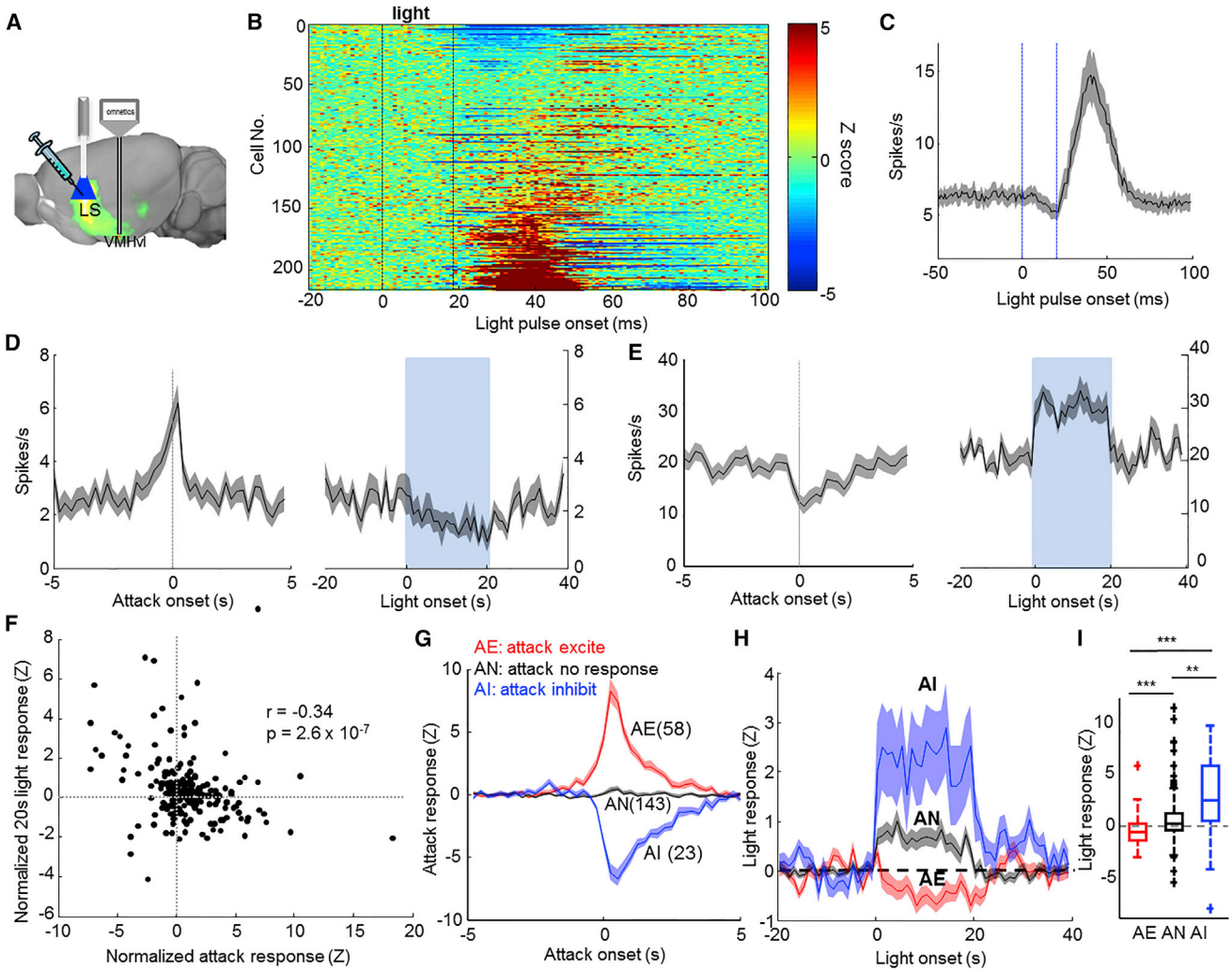

Figure 7. LS Activation Modulates Attack-Excited and Attack-Inhibited Cells Differentially

(A) VMHvl recording with LS optical stimulation.

(B) Z-score-normalized activity of all 224 cells aligned to light onset, sorted based on the average activity between 15 ms after light onset and 30 ms after light offset.

(C) Averaged PSTHs of all cells aligned to the light pulse onset. Vertical blue lines delimit the light-on period.

(D and E) PSTHs aligned to attack onset (left) and PTSHs aligned to 20 s light onset (right) from two example cells. Blue shades indicate the light pulsing period. The attack-excited cell (D) decreased spiking activity during the light pulsing period, whereas the attack-inhibited cell (E) increased activity.

(F) Averaged Z-scored activity during the 20 s light pulsing period is negatively correlated with the Z-scored attack response ($r = -0.34$, $p = 2.6 \times 10^{-7}$).

(G) Averaged Z-scored PSTHs of attack-excited (AE, red), attack-no-response (AN, black), and attack-inhibited (AI, blue) cells aligned to attack onset.

(H) Averaged Z-scored PSTHs of AE, AN, and AI cells aligned to the 20 s pulsed light onset.

(I) The activities of AE, AN, and AI cells during the 20 s light-on period are significantly different from each other (**$p < 0.01$, ***$p < 0.001$, t test). Error bars show means ± SEM.

Shading in (C)–(E), (G), and (H) shows ±SEM. See also Figure S5.

attack-inhibited cells were strongly excited by LS stimulation (one-sample t test, p = 0.01, n = 23; Figures 7G and 7H). Attack-nonresponsive cells were also excited by the light (one-sample t test, $p = 9.4 \times 10^{-5}$, n = 143), but the response was significantly weaker than that of attack-inhibited cells ($p = 5.9 \times 10^{-6}$, one-way ANOVA followed by multiple pair comparison) (Figure 7I).

Although attack was suppressed during light stimulation, this was unlikely to be the only cause of the firing rate change during light, given that the response was evident after each 20 ms light pulse, which was too short for any behavioral change (Figure 7B). Furthermore, the light-induced response remained qualitatively the same when we only considered trials when no attack occurred both before and during stimulation (Figure S5H). Excluding attack trials also did not change the negative correlation between the attack response and 20 s light-induced response (paired t test, r = –0.19, p = 0.006; Figure S5I). Taken together, these results suggest that LS could potentially modulate aggression through its interaction with both attack-excited and attack-inhibited cells in or around the

VMHvl by shifting the activity balance between these two populations.

DISCUSSION

In this study, we showed that the pathway from the LS to the VMHvl area is highly effective in modulating aggressive behaviors. Optogenetic activation of the GABAergic LS-VMH pathway terminated both natural inter-male attack and septal rage but had little effect on male-female mounting. Chronic in vivo optrode recording revealed that LS input suppressed attack-excited cells but surprisingly increased firing of attack-inhibited cells in and around the VMHvl. Thus, the LS can effectively modulate aggression by shifting the balance between attack-excited and attack-inhibited cells in the medial hypothalamus.

The LS-VMH Pathway Modulates Aggression

The rage response induced by septal lesion has been reported in numerous studies [5–7, 33]. More recently, $GABA_A$ receptor activation in the LS was shown to increase aggression in male hamsters, whereas $GABA_A$ receptor inactivation in the LS decreases maternal aggression in lactating mice [8, 9]. Consistent with the septal rage observed in previous studies, here we showed that LS-inactivation-induced attack differed from naturalistic territorial aggression in that the manipulated animals attacked both males and females whereas intact males rarely attack females. Thus, LS inactivation is likely to induce complex emotional and social recognition deficits beyond increased aggression. Indeed, the LS has been implicated in the regulation of affect, anxiety, the hypothalamic-pituitary-adrenal axis, and various aspects of social behaviors [26, 27, 34–38].

Despite the fact that the increased attack induced by the LS inactivation may be not purely territory related, activating the pathway from the LS to the VMHvl area suppressed natural inter-male aggression. Upon LS-VMH stimulation, the test animals quickly aborted an ongoing attack, but they continuously moved around the cage and investigated the intruder. Interestingly, LS-VMH stimulation had little effect on male-female mounting (Figures 3E, 3G, and 3I). During LS-VMH activation, the latency to stop mounting and the total percentage of time spent in mounting was not affected. Previous studies showed that although cells in the VMHvl were weakly excited during female investigation, VMHvl neuronal activity was largely unchanged or was even suppressed during advanced sexual behaviors [20]. In our current experiment, we presented a female mouse as an intruder to the recorded animal at the end of our recording sessions to further evaluate the involvement of the VMHvl cells in sexual behaviors. We found that 18/233 (7.7%) of VMHvl cells were significantly activated ($Z > 2$) during female investigation, while 42/233 (18.0%) cells were suppressed ($Z < -2$). In comparison, 27.9% (65/233) cells increased spiking activity and 11% (26/233) decreased activity while attacking males. Notably, among the female-excited cells, the majority (12/18) also significantly increased firing while attacking males, indicating that female-excited cells preferentially overlap with male-excited cells. Thus, as a population, the VMHvl is more responsive to males than to females and probably plays a more important role in male aggression than in sexual behaviors (Supplemental Experimental Procedures; Figures S6 and S7). Consistent with this hypothesis, reversible pharmacogenetic or optogenetic inhibition of VMHvl cells significantly suppressed aggression but failed to stop mounting and intromission [20, 22], although long-term perturbation, such as killing progesterone receptor-expressing cells in the area, reduced the number of intromissions and the duration of each intromission [21].

One limitation of the present study is that LS projection to the medial hypothalamus is not confined to the VMHvl. Areas lateral and ventral to the VMHvl including the juxtaventromedial region of the lateral hypothalamic area (LHAjv) and tuberal area (TU) also contain ChR2-EYFP fibers and may have been affected by the light. However, several lines of evidence suggest that LHAjv and TU might also play roles in aggression. Both LHAjv and TU are reciprocally connected with the VMHvl; show projection patterns similar to those of the VMHvl [39, 40]; show induction of Fos, a molecular surrogate of neural activity, after fighting [20]; and are parts of the "hypothalamic attack area" proposed in rats [41]. The main difference between the LHAjv and TU and the VMHvl is that the former two areas contain mostly GABAergic cells (see http://www.brain-map.org experiment ID: 72081554), whereas the cells in the VMHvl are nearly exclusively glutamatergic. One intriguing possibility is that some of the recorded attack-inhibited cells are actually located in the LHAjv and/or TU. The decreased activity of the GABAergic cells in the LHAjv/TU and increased activity of the glutamatergic cells in the VMHvl may work synergistically on downstream cells to initiate attack, while LS input may suppress attack by shifting the relative activity between these two populations. Future studies examining the influence of LS input on genetically tagged VMHvl or LHAjv/TU cells will help test this hypothesis.

Differential Responses of Attack-Inhibited and Attack-Excited Cells to LS Stimulation

Whole-cell in vitro recordings revealed that over 80% of VMHvl cells were inhibited by LS input. Optrode recording further demonstrated that the initial light-evoked response (within the first 15 ms) was predominantly inhibitory (Figures 6F and 6G). Thus, both attack-inhibited and attack-excited cells are likely to receive inhibitory inputs from the LS cells. However, their overall responses during the LS stimulation were significantly different. Whereas attack-excited cells were inhibited by LS optical stimulation, attack-inhibited cells showed an overall increase in firing rate due to the strong post-light excitation. This difference in light-induced activity change could be caused either by differences in biophysical properties of the cells or their placement in the neural network. A potential mechanism for the post-inhibitory rebound excitation is the activation of hyperpolarization-activated cyclic nucleotide-gated (HCN) channels and low voltage-activated T-type or L-type calcium channels [42]. In situ hybridization revealed that both T-type calcium channels and HCN1 are enriched in the VMHvl [43] (see also http://www.brain-map.org, experiments 71587822 and 77280561). Consistent with the expression of these ion channels in the VMHvl, we found that over 70% of VMHvl cells had rebound spikes after a brief hyperpolarizing current injection, and the number of rebound spikes was correlated with the magnitude of the initial sag, a signature of I_h current (Figures 5I–5K). Thus, attack-inhibited and attack-excited cells may differ in their

expression levels of HCN channels and/or T-type calcium channels, which could contribute to their difference in post-light excitatory responses. Under natural conditions, these differential responses may boost the impact of a transient inhibitory input onto the aggression circuit to effectively control behavior.

Alternatively, the post-light excitation observed in the attack-inhibited cells may not be cell autonomous but rather may be a circuit property. Since LS inputs appear to target both the VMHvl cells and cells surrounding the VMHvl (Figure 3C), during the LS stimulation, VMHvl cells could receive both direct inhibition and indirect disinhibition from the surrounding GABAergic neurons that collectively determine the changes in firing rate. These parallel and counter-acting projection patterns, one directly from the upstream region and one relayed through local GABAergic cells, are prevalent in the CNS [44], although they have not been studied in the context of the LS to medial hypothalamic projection and could represent an interesting direction for future studies.

EXPERIMENTAL PROCEDURES

Animals

Experimental mice were sexually experienced, singly housed, wild-type male C57BL/6N (12–24 weeks, Charles River) *Vgat*-ires-Cre and *Vglut2*-ires-Cre mice [29]. Intruders were either BALB/c males or C57BL/6 females (both 10–30 weeks). All procedures were approved by the Institutional Animal Care and Use Committee of NYU Langone Medical Center in accordance with NIH guidelines.

Stereotactic Injection and Implantation

For optogenetic manipulation, each wild-type animal was injected bilaterally with a total volume of 0.2–0.5 μl adeno-associated virus, which consisted of an equal mixture of AAV2/1 EF1α::DIO.hChR2(H134R).EYFP (2×10^{12} PFU/ml, UNC Vector Core), AAV2/1 CMV::CRE (2×10^{12} PFU/ml, University of Iowa Gene Transfer Vector Core), and either AAV2/1 CMV::LacZ (titer 1×10^{12} PFU/ml, UNC Vector Core) or AAV2/1 CAG.FLEX.tdTomato.WPRE.bGH (2×10^{12} PFU/ml, University of Pennsylvania Vector Core) into the LS (coordinates 0.5 mm AP, 0.45 mm ML, 3.0 mm DV). *Vgat*-ires-Cre mice were injected with 0.125–0.25 μl AAV2/1 EF1α::DIO.hChR2(H134R).EYFP. Control animals were injected with 0.25 μl of AAV2/1 CMV::PI.eGFP.WPRE.bGH (3×10^{12} PFU/ml, University of Pennsylvania Vector Core). Double cannulae were implanted 0.5 mm above LS injection sites, and 230 μm multimode optic fibers with 1.25 mm ferrules were implanted 0.8 mm above the VMHvl area (–1.7 mm AP, 0.68 mm ML, 5.0 mm DV) to allow light delivery. For optrode recording, a movable optrode containing sixteen 13 μm tungsten microwires and one 105 μm multimode optic fiber (Thorlabs) was implanted immediately above the putative VMHvl and a 230 μm optic fiber was implanted above the LS. For LS inactivation, 0.2–0.3 μl of 0.33 mg/ml muscimol (Sigma) (Figure 1) or 8% lidocaine and 0.1 mM TTX mixture (Figure 4) in saline were injected into the LS through the implanted double cannulae.

Optogenetic Activation

For LS stimulation, experiments started 2–4 weeks after injection. For LS-VMHvl stimulation, experiments started 4–8 weeks after injection. During the test, male BALB/c intruders were introduced into the resident's cage, and light stimulations (20 ms, 20 Hz, 1–3 mW, 20 s), interleaved with no-light sham stimulations, were initiated after spontaneously occurring attacks were observed. The same stimulation protocol was used for mounting behavioral tests in the presence of a C57BL/6 female.

In Vitro Slice Recording

Acute slices of the VMHvl were prepared from adult C57Bl/6N mice that were used in the optogenetic experiments and *Vglut2*-ires-Cre × Ai6 mice injected with 0.25 μl AAV2/1 EF1α::DIO.hChR2(H134R).EYFP (2×10^{12} PFU/ml, UNC Vector Core) into the LS. Somatic whole-cell recordings were made from VMHvl neurons in either voltage-clamp or current-clamp mode with a Multiclamp 700B amplifier (Molecular Devices).

In Vivo Optrode Recording

During optrode recording, we introduced a male intruder and then delivered blue light first through the optrode (5–10 repetitions of 20 s, 20 ms, 5 Hz pulses) and then through the implanted optic fiber at the LS (8–10 repetitions of 20 s, 20 ms, 5 Hz pulses). The light delivery is independent of ongoing behaviors. After removing the male intruder, we then introduced the female intruder for 10 min without any light delivery. Acquired spikes were sorted using an Offline Sorter (Plexon). All behavioral and electrophysiological analyses were performed using customized MATLAB software [45, 46].

See Supplemental Experimental Procedures for additional methods.

SUPPLEMENTAL INFORMATION

Supplemental Information includes seven figures and Supplemental Experimental Procedures and can be found with this article online at http://dx.doi.org/10.1016/j.cub.2015.12.065.

AUTHOR CONTRIBUTIONS

D.L. conceived the project, designed and funded experiments, analyzed data, and wrote the manuscript. L.C.W. performed research, analyzed data, and co-wrote the manuscript. L.W. performed parts of optogenetic experiments and histological analysis and co-wrote the paper. G.C., H.B., and X.Y. performed parts of optogenetic experiments. J.D. performed all slice recording experiments. T. Yumita performed parts of in vivo recording experiments. T. Yamaguchi performed parts of histological analysis. B.C.C. and J.E.F. assisted in vivo recordings. R.C.F. supervised slice recording experiments.

ACKNOWLEDGMENTS

We would like to thank B. Lowell for providing the *Vgat*-ires-Cre and *Vglut2*-ires-Cre mice, G. Fishell for providing RCE:loxP mice, all D.L. lab members for helpful discussions, L. Wang for assistance with genotyping, and P. Hare for editorial comments. This work was supported by the Esther A. & Joseph Klingenstein Fund (D.L.), Whitehall Foundation (D. L.), Sloan Foundation (D.L.), McKnight Foundation (D.L.), Mather's Foundation (D.L.), and National Institutes of Health grant 1R01MH101377 (D.L.).

Received: November 24, 2015
Revised: December 17, 2015
Accepted: December 22, 2015
Published: February 11, 2016

REFERENCES

1. Bard, P. (1928). A diencephalic mechanism for the expression of rage with special reference to the sympathetic nervous system. Am. J. Physiol. *84*, 490–515.
2. Spiegel, E.A., Miller, H.R., and Oppenheimer, M.J. (1940). Forebrain and rage reactions. J. Neurophysiol. *3*, 538–548.
3. Goodson, J.L., Evans, A.K., and Soma, K.K. (2005). Neural responses to aggressive challenge correlate with behavior in nonbreeding sparrows. Neuroreport *16*, 1719–1723.
4. Zeman, W., and King, F.A. (1958). Tumors of the septum pellucidum and adjacent structures with abnormal affective behavior: an anterior midline structure syndrome. J. Nerv. Ment. Dis. *127*, 490–502.
5. Albert, D.J., and Chew, G.L. (1980). The septal forebrain and the inhibitory modulation of attack and defense in the rat. A review. Behav. Neural Biol. *30*, 357–388.
6. Slotnick, B.M., McMullen, M.F., and Fleischer, S. (1973). Changes in emotionality following destruction of the septal area in albino mice. Brain Behav. Evol. *8*, 241–252.

7. Potegal, M., Blau, A., and Glusman, M. (1981). Effects of anteroventral septal lesions on intraspecific aggression in male hamsters. Physiol. Behav. *26*, 407–412.
8. McDonald, M.M., Markham, C.M., Norvelle, A., Albers, H.E., and Huhman, K.L. (2012). GABAA receptor activation in the lateral septum reduces the expression of conditioned defeat and increases aggression in Syrian hamsters. Brain Res. *1439*, 27–33.
9. Lee, G., and Gammie, S.C. (2009). GABA(A) receptor signaling in the lateral septum regulates maternal aggression in mice. Behav. Neurosci. *123*, 1169–1177.
10. Ramirez, J.M., Salas, C., and Portavella, M. (1988). Offense and defense after lateral septal lesions in Columba livia. Int. J. Neurosci. *41*, 241–250.
11. Goodson, J.L., Eibach, R., Sakata, J., and Adkins-Regan, E. (1999). Effect of septal lesions on male song and aggression in the colonial zebra finch (Taeniopygia guttata) and the territorial field sparrow (Spizella pusilla). Behav. Brain Res. *98*, 167–180.
12. Siegel, A., and Skog, D. (1970). Effects of electrical stimulation of the septum upon attack behavior elicited from the hypothalamus in the cat. Brain Res. *23*, 371–380.
13. Potegal, M., Blau, A., and Glusman, M. (1981). Inhibition of intraspecific aggression in male hamsters by septal stimulation. Physiol. Psychol. *9*, 213–218.
14. Risold, P.Y., and Swanson, L.W. (1997). Connections of the rat lateral septal complex. Brain Res. Brain Res. Rev. *24*, 115–195.
15. Blume, H.W., Pittman, Q.J., Lafontaine, S., and Renaud, L.P. (1982). Lateral septum-medial hypothalamic connections: an electrophysiological study in the rat. Neuroscience *7*, 2783–2792.
16. Lammers, J.H., Kruk, M.R., Meelis, W., and van der Poel, A.M. (1988). Hypothalamic substrates for brain stimulation-induced attack, teeth-chattering and social grooming in the rat. Brain Res. *449*, 311–327.
17. Lipp, H.P., and Hunsperger, R.W. (1978). Threat, attack and flight elicited by electrical stimulation of the ventromedial hypothalamus of the marmoset monkey Callithrix jacchus. Brain Behav. Evol. *15*, 260–293.
18. Siegel, A., and Pott, C.B. (1988). Neural substrates of aggression and flight in the cat. Prog. Neurobiol. *31*, 261–283.
19. Siegel, A., Roeling, T.A.P., Gregg, T.R., and Kruk, M.R. (1999). Neuropharmacology of brain-stimulation-evoked aggression. Neurosci. Biobehav. Rev. *23*, 359–389.
20. Lin, D., Boyle, M.P., Dollar, P., Lee, H., Lein, E.S., Perona, P., and Anderson, D.J. (2011). Functional identification of an aggression locus in the mouse hypothalamus. Nature *470*, 221–226.
21. Yang, C.F., Chiang, M.C., Gray, D.C., Prabhakaran, M., Alvarado, M., Juntti, S.A., Unger, E.K., Wells, J.A., and Shah, N.M. (2013). Sexually dimorphic neurons in the ventromedial hypothalamus govern mating in both sexes and aggression in males. Cell *153*, 896–909.
22. Lee, H., Kim, D.W., Remedios, R., Anthony, T.E., Chang, A., Madisen, L., Zeng, H., and Anderson, D.J. (2014). Scalable control of mounting and attack by Esr1+ neurons in the ventromedial hypothalamus. Nature *509*, 627–632.
23. Falkner, A.L., Dollar, P., Perona, P., Anderson, D.J., and Lin, D. (2014). Decoding ventromedial hypothalamic neural activity during male mouse aggression. J. Neurosci. *34*, 5971–5984.
24. Millhouse, O.E. (1973). The organization of the ventromedial hypothalamic nucleus. Brain Res. *55*, 71–87.
25. Millhouse, O.E. (1973). Certain ventromedial hypothalamic afferents. Brain Res. *55*, 89–105.
26. Sheehan, T.P., Chambers, R.A., and Russell, D.S. (2004). Regulation of affect by the lateral septum: implications for neuropsychiatry. Brain Res. Brain Res. Rev. *46*, 71–117.
27. Anthony, T.E., Dee, N., Bernard, A., Lerchner, W., Heintz, N., and Anderson, D.J. (2014). Control of stress-induced persistent anxiety by an extra-amygdala septohypothalamic circuit. Cell *156*, 522–536.
28. Kita, T., Nishijo, H., Eifuku, S., Terasawa, K., and Ono, T. (1995). Place and contingency differential responses of monkey septal neurons during conditional place-object discrimination. J. Neurosci. *15*, 1683–1703.
29. Vong, L., Ye, C., Yang, Z., Choi, B., Chua, S., Jr., and Lowell, B.B. (2011). Leptin action on GABAergic neurons prevents obesity and reduces inhibitory tone to POMC neurons. Neuron *71*, 142–154.
30. Zhao, C., Eisinger, B., and Gammie, S.C. (2013). Characterization of GABAergic neurons in the mouse lateral septum: a double fluorescence in situ hybridization and immunohistochemical study using tyramide signal amplification. PLoS ONE *8*, e73750.
31. Jennings, J.H., Sparta, D.R., Stamatakis, A.M., Ung, R.L., Pleil, K.E., Kash, T.L., and Stuber, G.D. (2013). Distinct extended amygdala circuits for divergent motivational states. Nature *496*, 224–228.
32. Tong, Q., Ye, C., McCrimmon, R.J., Dhillon, H., Choi, B., Kramer, M.D., Yu, J., Yang, Z., Christiansen, L.M., Lee, C.E., et al. (2007). Synaptic glutamate release by ventromedial hypothalamic neurons is part of the neurocircuitry that prevents hypoglycemia. Cell Metab. *5*, 383–393.
33. Brady, J.V., and Nauta, W.J. (1953). Subcortical mechanisms in emotional behavior: affective changes following septal forebrain lesions in the albino rat. J. Comp. Physiol. Psychol. *46*, 339–346.
34. Herman, J.P., and Cullinan, W.E. (1997). Neurocircuitry of stress: central control of the hypothalamo-pituitary-adrenocortical axis. Trends Neurosci. *20*, 78–84.
35. Sodetz, F.J., and Bunnell, B.N. (1970). Septal ablation and the social behavior of the golden hamster. Physiol. Behav. *5*, 79–88.
36. Numan, R. (2000). The Behavioral Neuroscience of the Septal Region (Springer).
37. Mesic, I., Guzman, Y.F., Guedea, A.L., Jovasevic, V., Corcoran, K.A., Leaderbrand, K., Nishimori, K., Contractor, A., and Radulovic, J. (2015). Double Dissociation of the Roles of Metabotropic Glutamate Receptor 5 and Oxytocin Receptor in Discrete Social Behaviors. Neuropsychopharmacology *40*, 2337–2346.
38. Ferguson, J.N., Young, L.J., and Insel, T.R. (2002). The neuroendocrine basis of social recognition. Front. Neuroendocrinol. *23*, 200–224.
39. Hahn, J.D., and Swanson, L.W. (2015). Connections of the juxtaventromedial region of the lateral hypothalamic area in the male rat. Front. Syst. Neurosci. *9*, 66.
40. Canteras, N.S., Simerly, R.B., and Swanson, L.W. (1994). Organization of projections from the ventromedial nucleus of the hypothalamus: a Phaseolus vulgaris-leucoagglutinin study in the rat. J. Comp. Neurol. *348*, 41–79.
41. Kruk, M.R., Van der Poel, A.M., Meelis, W., Hermans, J., Mostert, P.G., Mos, J., and Lohman, A.H.M. (1983). Discriminant analysis of the localization of aggression-inducing electrode placements in the hypothalamus of male rats. Brain Res. *260*, 61–79.
42. Robinson, R.B., and Siegelbaum, S.A. (2003). Hyperpolarization-activated cation currents: from molecules to physiological function. Annu. Rev. Physiol. *65*, 453–480.
43. Qiu, J., Bosch, M.A., Jamali, K., Xue, C., Kelly, M.J., and Rønnekleiv, O.K. (2006). Estrogen upregulates T-type calcium channels in the hypothalamus and pituitary. J. Neurosci. *26*, 11072–11082.
44. Roux, L., and Buzsáki, G. (2015). Tasks for inhibitory interneurons in intact brain circuits. Neuropharmacology *88*, 10–23.
45. Dollar, P., Welinder, P., and Perona, P. (2010). Cascaded pose regression. Proceedings of the 2010 IEEE Conference on Computer Vision and Pattern Recognition *2010*, 1078–1085.
46. Burgos-Artizzu, X.P., Dollár, P., Lin, D., Anderson, D.J., and Perona, P. (2012). Social behavior recognition in continuous videos. Proceedings of the 2012 IEEE Conference on Computer Vision and Pattern Recognition *2012*, 1322–1329.

